CrystEngComm

Accepted Manuscript

ROYAL SOCIETY
OF CHEMISTRY

www.rsc.org/crystengcomm

Journal Name

Cite this: DOI: 10.1039/c0xx00000x

www.rsc.org/xxxxxx

ARTICLE TYPE

Two robust metal-organic frameworks with uncoordinated N atoms for CO_2 adsorption

Guo-Jian Ren, Yan-Qing Liu, Tong-Liang Hu* and Xian-He Bu

Received (in XXX, XXX) Xth XXXXXXXXX 20XX, Accepted Xth XXXXXXXXX 20XX
DOI: 10.1039/b000000x

Two highly porous metal-organic frameworks are successfully constructed through the assembling of Co/Ni ions and mixed ligands. Contributed to uncoordinated tetrazolate N atoms of ligand, two complexes show high CO_2 adsorption capacities, serving as potential CO_2 adsorption materials.

Due to very high surface area, chemical tunability and tailorability, metal-organic framework (MOFs), as one kind of emerging porous material, exhibit multifunctional applications in sensors, catalysis, drug delivery, gas storage, in particular, selective CO_2 adsorption.[1-3] It is well known that the increase of anthropogenic CO_2 emissions to the atmosphere is believed to be responsible for global warming. Thus, the development of high-powered carbon capture and storage is important for environment.[4,5]

Some strategies have been proposed to enhance the interaction between the MOFs and CO_2 molecules, and increase the uptake amount of CO_2. One effective approach for strong CO_2 binding affinity and high adsorption amount is existence of amides in the pore wall of MOFs architecture, another efficient method is the introduction of unsaturated metal sites in the construction of MOFs, and the third strategy is rational choice of ligand with uncoordinated N atoms.[6-8]

Motivated by the third strategy, N-rich ligand is adopted to build porous MOFs for the adsorption of CO_2. It is well known that MOFs are always built with in-built functional properties using the secondary building unit (SBU) approach, which utilizes pre-selected organic and inorganic SBUs.[9] With judicious chosen of SBUs, it is feasible to possess the frameworks with proper geometry, shape, directionality and underlying nets.[10]

Herein, we choose 5-(4-pyridyl)-tetrazolate (4-Ptz) with two different coordinated functional group as primary ligand, and terephthalic acid (H_2BDC) as auxiliary ligand. Fortunately, two robust complexes with **ncb** net are successfully constructed by reasonably self-assembling. Compared with the reported results,[8a,8b,16,17b,18c] title complexes show improved CO_2 adsorption capacity.

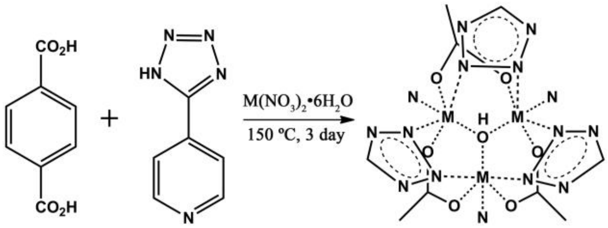

Scheme 1 Construction of complexes **1** and **2**.

Solvothermal reaction of $Co(NO_3)_2·6H_2O$ or $Ni(NO_3)_2·6H_2O$, terephthalic acid (H_2BDC) and 4-Ptz in *N*,*N*´-dimethylformamide (DMF) for three days gave two complexes **1** $[Co_3OH(BDC)_{1.5}(4\text{-}Ptz)_3](DMF)_2(DMA)_1$ (DMA = Dimethylamine cation) and **2** $[Ni_3OH(BDC)_{1.5}(4\text{-}Ptz)_3](DMF)_{5.4}$. Due to the isomorphous characters of **1** and **2**, the structure of **1** is described in detail. Complex **1** crystalizes in cubic space group *I*-43*m*, and the asymmetric unit contains 1/2 Co ion, 1/6 μ_3-O, 1/4 BDC and 1/2 4-Ptz. Co1 ion reveals six-coordinated geometrical configuration, which is ligated by 2 N atoms of tetrazole units, 2 O atoms from carboxylate groups, 1 N atom of pyridine group and 1 μ_3-OH O atom. The O2 atom linking three Co ions in a μ_3 mode locates a position with the 3m symmetry, and the Co1 and N1 lie a site with m symmetry. Three Co ions are chelated by three carboxylate groups of BDC and three tetrazole units from 4-Ptz, and axially coordinated by three pyridine N atoms of 4-Ptz. So the Co_3OH SBU is linked by six 4-Ptz and three BDC ligands, showing the 9-connected mode. It should be noted that the chelated mode of tetrazole unit in 4-Ptz is similar with carboxylate group as shown in literatures,[11] giving the probability for the construction of 9-connected SBU. When the SBU was regard as node, the framework can be simplified as the **ncb** net with the point symbol $\{3^{12}.\ 4^{12}.\ 5^{12}\}$. Compared with other reported **ncb** net (Co-OH-Co 119º), the Co-OH-Co angle is 116.43 º.[12,13] The oxidation states of the three Co ions are confirmed through bond valence sum rule, indicating three Co^{II} ions in the estimated formula. Magnetic measurements are performed in order to determine the oxidation states of the Co ions. As shown in the electronic supporting information (ESI), the obtained experimental value C_{exp} of 10.10 $cm^3\ K\ mol^{-1}$ as well as $\chi_m T$ product (7.94 $cm^3\ K\ mol^{-1}$) at 300 K displays consistence with the reported result, corresponding to the presence of 3 Co^{2+} ($S = 3/2$).[14] Hence, the negetive charge of framework is balanced by free DMA. Different with **1**, the trinuclear Ni cluster in **2**

School of Materials Science and Engineering, National Institute for Advanced Materials, Collaborative Innovation Center of Chemical Science and Engineering(Tianjin), Nankai University, Tianjin 300071, P. R. China. Fax: +86-22-23502458. E-mail: tlhu@nankai.edu.cn

†Electronic Supplementary Information (ESI) available: [materials and general methods, bond valence sum, magnetic measurement, TGA, IR spectra]. See DOI: 10.1039/b000000x/

contains 2 Ni^{2+} and 1 Ni^{3+} per formula unit which is also determined through bond valence sum rule, and magnetic data also prove that in ESI.[15]

Four Co_3OH SBUs link with six BDC ligands to form the tetrahedron cage, and the interior hole of tetrahedron is about 10.0 Å in diameter (ignoring van der waals radius). On the other hand, the trigonal pyramid is constructed by the connection of three BDC and three 4-Ptz ligands together with four Co_3OH, forming the hole with 7.2 Å in diameter. A tetrahedron is surrounded by four trigonal pyramids through face-shared connection as shown in Fig. 1d. By the packing of two kinds of polyhedrons, the three-dimensional channel is formed in the complex **1** with the diameter of 10 Å. One important feature is that two N atoms of tetrazole are uncoordinated, giving the potential application toward CO_2 adsorption.

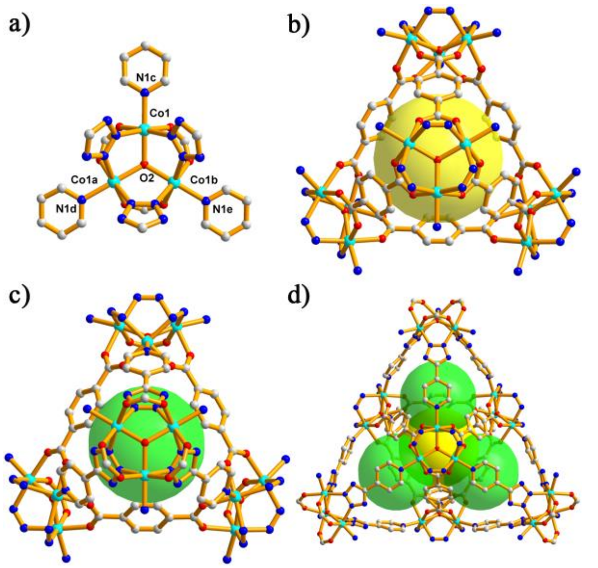

Fig. 1 a) The coordination configuration of trinuclear cluster in complex **1** (grey: C, blue: N, red: O, turquoise: Co, H atoms are omitted for clarity), symmetry codes: a = -z+1, -x+1, y; b = -y+1, z, -x+1; c = -z+1/2, -y+1/2, x-1/2; d = -x+1.5, z+0.5, -y+0.5; e = -x+1.5, -y+0.5, z+0.5, b) the presentation of tetrahedron cage, c) the exhibition of triangular pyramidal cage, d) face-shared connection between tetrahedron and triangular pyramidal cage.

X-ray powder diffraction (XRPD) is used to check the purity of the title complexes. As shown in Fig. 2, all the peaks displayed in the measured patterns at room temperature of **1** and **2** match closely with those in the simulated patterns generated from single-crystal diffraction data, which indicates single phases of them are formed. As shown in Fig. S4, the thermogravimetric analysis (TGA) curves of **1** shows two obvious platforms. Before the first platform, it indicates that the lattice guest molecules in the framework are gradually lost, corresponding to two DMF and one dimethylamine. When the temperature reaches 300 ºC, the framework begins to decompose. As the temperature reaches 450 ºC, the framework decomposes completely. As for complex **2** (Fig. S5), the lattice solvent molecules in the framework are gradually removed until the temperature reach 242 ºC corresponding to 5.4 DMF. When the temperature reaches 430 ºC, the framework decomposes completely.

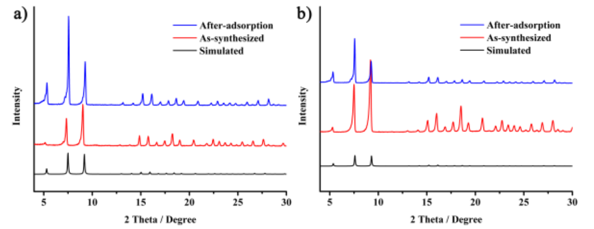

Fig. 2 The PXRD patterns of **1** and **2** in the condition of as-synthesized and after-adsorption.

Highly porous architecture feature and good stability make **1** and **2** the candidates for gas adsorption materials. The N_2 adsorption measurements are performed in order to evaluate the porosity of two complexes. The N_2 adsorption isotherm of **1** and **2** reveal classic type I plot as shown in Fig. 3, indicating the microporous character of two complexes. The uptake amounts are 377.5 and 368.6 cm^3/g, corresponding to the BET surface 1221 and 1192 m^2/g (Langmuir surface: 1619 and 1569 m^2/g), respectively. The fit of the adsorption data by using the H-K (Horvath–Kawazoe) method give the pore width distribution of **1** and **2** (Fig. S9 and Fig. S10). Two complexes show similar pore volumes through the N_2 adsorption isotherms (0.58 cm^3/g for **1** and 0.56 cm^3/g for **2**), slightly less than the pore volumes estimated from the single-crystal structure (about 0.66 cm^3/g for both **1** and 0.64 cm^3/g for **2**).

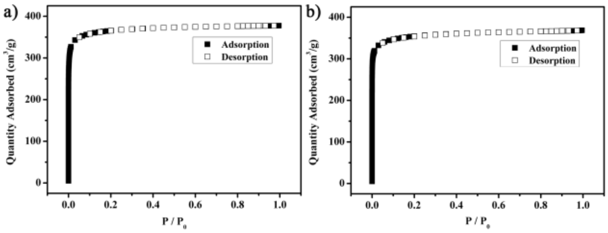

Fig. 3 N_2 adsorption isotherms of **1** (a) and **2** (b).

The feature of the permanent porosity of **1** and **2** encourages us to evaluate their potential application on CO_2 adsorption properties. The CO_2 adsorption measurements of **1** and **2** are performed at 273 K, 298 K and 323 K, respectively. As shown in Fig. 4, the uptake amounts of **1** are 114.8, 56.8 and 33.0 cm^3/g, and 126.8, 51.8, and 29.8 cm^3/g for **2**. The initial Qst of CO_2 adsorption is 26.0 kJ/mol in **1**, and 24.0 kJ/mol for **2**. Compared with the reported examples with **ncb** net, the adsorption amount of **1** and **2** is much higher,[16] which could contribute to the enhanced interaction between adsorbed CO_2 molecules and uncoordinated N atoms with lone electron pairs from N-rich aromatic rings.[17] The amount adsorbed is comparable with other reported MOFs with similar uncoordinated N atoms, which is comparable with CPF-6[8b] and IFMC-1[17b] (98 and 91.4 cm^3/g at 273 K) and higher than MAF-25 and MAF-26.[8a]

Due to the high CO_2 adsorption amount at 1 atm, the high pressure adsorption measurements of **1** and **2** are performed. The uptake amounts at 15 bars are 41.0 and 40.8 wt%, corresponding to 208.7 and 207.7 cm^3/g, respectively, which is inferior to highly porous MIL-101 (44.2 wt%), comparable with classic HKUST-1 (42.8 wt%) and higher than ZIF-8 (35.0 wt%).[18]

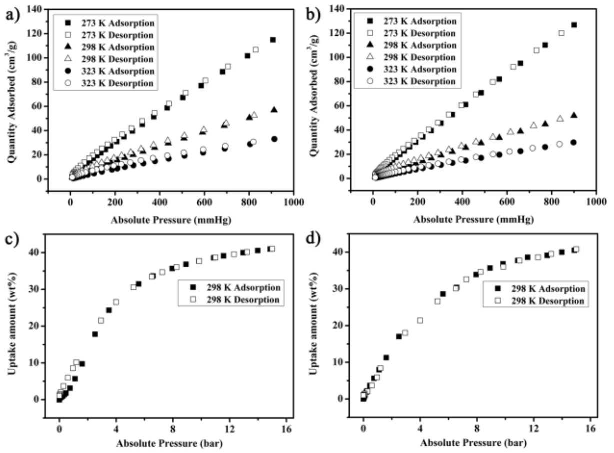

Fig. 4 a) CO_2 adsorption isotherms of complex **1** at 1 atm, b) CO_2 adsorption isotherms of complex **2** at 1 atm, c) high pressure CO_2 adsorption isotherm of **1**, d) high pressure CO_2 adsorption isotherm of **2**.

After the above-mentioned adsorption operation, the PXRD of samples **1** and **2** are performed. The good match of patterns of the after-adsorption samples with the simulated patterns from the single-crystal structures suggests the crystal persistence of complexes **1** and **2**. The robust features of both complexes are further conformed.

In conclusion, two highly porous MOFs, containing uncoordinated tetrazolate nitrogen sites, are successfully constructed through solvothermal reaction. Both complexes show high CO_2 adsorption amounts which could be served as the high efficient adsorption materials.

This work was supported by 973 Program of China (2014CB845600), the National Science Foundation of China (21371102 and 21421001), and MOE Innovation Team of China (IRT13022).

Notes and references

Synthesis of **1**: A mixture of $Co(NO_3)_2\cdot6H_2O$ (0.5 mmol), H_2BDC (0.5 mmol), 4-Ptz (0.5 mmol) and $LiNO_3$ (0.5 mmol) in 12 mL DMF was sealed in a 20 ml Teflon-lined autoclave and heated at 150 °C for 48 hours. After that, the reaction vessel was cooled to room temperature in 24 h. Red crystals were collected by filtration, washed with DMF and dried in air (yield: 20-25% based on $Co(NO_3)_2\cdot6H_2O$). Though Li^+ was not solved through X-ray single crystal analysis, the content of Li^+ in **1** was 0.45% as determined by ICP, and the counter ion was NO_3^- which was demonstrated through IR spectrum. Element analysis (%): Calculated: C, 42.63; N, 23.55; H, 3.73. Found: C, 42.33; N, 23.25; H, 3.99.

Synthesis of **2** is similar with **1** except that the $Co(NO_3)_2\cdot6H_2O$ is replaced by $Ni(NO_3)_2\cdot6H_2O$. The content of Li^+ in **2** was 0.43% as determined by ICP. Element analysis (%): Calculated: C, 43.65; N, 22.44; H, 4.38. Found: C, 43.32; N, 22.12; H, 4.59.

$LiNO_3$, as structure-induced reagent, was added in the synthesis process. Complexes **1** and **2** cannot obtain without the $LiNO_3$.

Crystal data for **1**: $C_{38}H_{40}Co_3N_{18}O_9$, *M*r = 1069.67, Cubic, a = 23.570 (3) Å, V = 13095 (3) Å^3, T= 113.15 K, space group *I*-43*m*, Z = 8, μ = 0.803 mm^{-1}, R_{int} = 0.3068. The final R_1 value was 0.0661 (I > 2σ(I)). The final wR_2 value was 0.1594 (I > 2σ(I)). The final R_1 value was 0.0762 (all data). The final wR_2 value was 0.1647 (all data). The goodness of fit on F2 was 1.040. CCDC No: 1400193.

Crystal data for **2**: $C_{46.25}H_{55.75}Ni_3N_{20.38}O_{12.38}$, *M*r = 1271.24, Cubic, a = 23.290 (3) Å, V = 12633 (3) Å^3, T= 113.15 K, space group *I*-43*m*, Z = 8, μ = 0.955 mm^{-1}, R_{int} = 0.0731. The final R_1 value was 0.0289 (I > 2σ(I)). The final wR_2 value was 0.0762 (I > 2σ(I)). The final R_1 value was 0.0294 (all data). The final wR_2 value was 0.0765 (all data). The goodness of fit on F2 was 1.111. CCDC No: 1400192.

1 (a) Z. Hu, B. J. Deibert and J. Li, *Chem. Soc. Rev.*, 2014, **43**, 5815-5840; (b) T. A. Makal, J. R. Li, W. G. Lu and H. C. Zhou, *Chem. Soc. Rev.*, 2012, **41**, 7761-7779; (c) L. Q. Ma, C. Abney and W. B. Lin, *Chem. Soc. Rev.*, 2009, **38**, 1248-1256; (d) S. Horike, D. Umeyama and S. Kitagawa, *Acc. Chem. Res.*, 2013, **46**, 2376-2384; (e) Q. Chen, Z. Chang, W. C. Song, H. Song, H. B. Song, T. L. Hu and X. H. Bu, *Angew. Chem., Int. Ed.*, 2013, **52**, 11550-11553; (f) H. Wang, T. L. Hu, R. M. Wen, Q. Wang and X. H. Bu, *J. Mater. Chem. B*, 2013, **1**, 3879-3882; (g) D. S. Li, Y. P. Wu, J. Zhao, J. Zhang and J. Y. Lu, *Coord. Chem. Rev.*, 2014, **261**, 1-27; (h) J. Zhao, Y. Wang, W. Dong, Y.Wu, D. Li, B. Liu and Q. Zhang, *Chem. Commun.*, 2015, **51**, 9479-9482.

2 (a) J. Liu, P. K. Thallapally, B. P. McGrail, D. R. Brown and J. Liu, *Chem. Soc. Rev.*, 2012, **41**, 2308-2322; (b) K. Sumida, D. L. Rogow, J. A. Mason, T. M. McDonald, E. D. Bloch, Z. R. Herm, T. H. Bae and J. R. Long, *Chem. Rev.*, 2012, **112**, 724-781; (c) Z. X. Xu, Y. X. Tan, H. R. Fu, J. Liu and J. Zhang, *Inorg. Chem.*, 2014, **53**, 12199-12204; (d) Y. Q. Chen, G. R. Li, Z. Chang, Y. K. Qu, Y. H. Zhang and X. H. Bu, *Chem. Sci.*, 2013, **4**, 3678-3682; (e) S. Xiang, Y. He, Z. Zhang, H. Wu, W. Zhou, R. Krishna, B. Chen, *Nat. Commun.*, 2012, **3**, 954.

3 (a) C. E. Wilmer, O. K. Farha, Y. S. Bae, J. T. Hupp and R. Q. Snurr, *Energy Environ. Sci.*, 2012, **5**, 9849-9856; (b) Y. Xie, H. Yang, Z. U. Wang, Y. Liu, H. C. Zhou and J. R. Li, *Chem. Commun.*, 2014, **50**, 563-565; (c) D. Tian, Q. Chen, Y. Li, Y. H. Zhang, Z. Chang and X. H. Bu, *Angew. Chem., Int. Ed.*, 2014, **53**, 837-841; (d) Z. Zhang, Z. Yao, S. Xiang and B. Chen, *Energy Environ. Sci.*, 2014, **7**, 2868.

4 (a) C. D. Keeling, T. P. Whorf, M. Wahlen and J. van der Plichtt, *Nature*, 1995, **375**, 666-670; (b) T. R. Karl and K. E. Trenberth, *Science*, 2003, **302**, 1719-1723; (c) R. S. Haszeldine, *Science*, 2009, **325**, 1647-1652.

5 (a) B. Arstad, R. Blom, O. Swang, *J. Phys. Chem. A*, 2007, **111**, 1222-1228; (b) G. T. Rochelle, *Science*, 2009, **325**, 1652-1654.

6 (a) R. Vaidhyanathan, S. S. Iremonger, G. K. H. Shimizu, P. G. Boyd, S. Alavi and T. K. Woo, *Science*, 2010, **330**, 650-653; (b) Y. Hu, W. M. Verdegaal, S. H. Yu and H. L. Jiang, *ChemSusChem*, 2014, **7**, 734-737; (c) Q. Yan, Y. Lin, C. Kong and L. Chen, *Chem. Commun.*, 2013, **49**, 6873-6875.

7 (a) D. Britt, H. Furukawa, B. Wang, T. G. Glover and O. M. Yaghi, *Proc. Natl. Acad. Sci. U. S. A.*, 2009, **106**, 20637-20640; (b) Y. Huang, B. Zhang, J. Duan, W. Liu, X. Zheng, L. Wen, X. Ke, D. Li, *Cryst. Growth Des.*, 2014, **14**, 2866-2872; (c) C. R. Wade, M. Dincă, *Dalton Trans.*, 2012, **41**, 7931-7938.

8 (a) J. B. Lin, J. P. Zhang and X. M. Chen, *J. Am. Chem. Soc.*, 2010, **132**, 6654-6656; (b) Q. Lin, T. Wu, S. T. Zheng, X. Bu and P. Feng, *J. Am. Chem. Soc.*, 2012, **134**, 784-787; (c) P. Pachfule, R. Banerjee, *Cryst. Growth Des.*, 2011, **11**, 5176-5181.

9 (a) Z. J. Lin, J. Lü, M. C. Hong and R. Cao, *Chem. Soc. Rev.*, 2014, **43**, 5867-5895; (b) Y. Yan, S. H. Yang, A. J. Blake, and M. Schröder, *Acc. Chem. Res.*, 2014, **47**, 296-307; (c) D. J. Tranchemontagne, J. L. Mendoza-Cortés, M. O'Keeffe and O. M. Yaghi, *Chem. Soc. Rev.*, 2009, **38**, 1257-1283.

10 (a) O. K. Farha, I. Eryazici, N. C. Jeong, B. G. Hauser, C. E. Wilmer, A. A. Sarjeant, R. Q. Snurr, S. T. Nguyen, A. Ö. Yazaydın and J. T. Hupp, *J. Am. Chem. Soc.*, 2012, **134**, 15016-15021; (b) J. F. Eubank, F. Nouar, R. Luebke, A. J. Cairns, L. Wojtas, M. Alkordi, T. Bousquet, M. R. Hight, J. Eckert, J. P. Embs, P. A. Georgiev and M. Eddaoudi, *Angew. Chem. Int. Ed.*, 2012, **51**, 10099-10103; (c) Y. S. Wei, K. J. Chen, P. Q. Liao, B. Y. Zhu, R. B. Lin, H. L. Zhou, B. Y. Wang, W. Xue, J. P. Zhang and X. M. Chen, *Chem. Sci.*, 2013, **4**, 1539-1546.

11 (a) S. Goswami, S. Sanda and S. Konar, *CrystEngComm*, 2014, **16**, 369-374; (b) B. Y. Wu, C. I. Yang, M. Nakano and G. H. Lee, *Dalton Trans.*, 2014, **43**, 47-50.

12 (a) Y. B. Zhang, W. X. Zhang, F. Y. Feng, J. P. Zhang, X. M. Chen, *Angew. Chem. Int. Ed.*, 2009, **48**, 5287-5290; (b) X. Zhao, X. Bu, T.

Wu, S. T. Zheng, L. Wang, P. Feng, *Nat. Commun.*, 2013, **4**, 2344.

13 Y. B. Zhang, H. L. Zhou, R. B. Lin, C. Zhang, J. B. Lin, J. P. Zhang, X. M. Chen, *Nat. Commun.*, 2012, **3**, 642.

14 Q. Chen, J. B. Lin, W. Xue, M. H. Zeng and X. M. Chen, *Inorg. Chem.*, 2011, **50**, 2321-2328.

15 (a) J. H. Jia, X. Lin, C. Wilson, A. J. Blake, N. R. Champness, P. Hubberstey, G. Walker, E. J. Cussen and M. Schröder, *Chem. Commun.*, 2007, 840-842; (b) Y. B. Zhang, W. X. Zhang, F. Y. Feng, J. P. Zhang and X. M. Chen, *Angew. Chem., Int. Ed.*, 2009, **48**, 5287-5290.

16 (a) G. Jiang, T. Wu, S. T. Zheng, X. Zhao, Q. Lin, X. Bu and P. Feng, *Cryst. Growth Des.*, 2011, **11**, 3713-3716; (b) E. Yang, Z. S. Liu, S. Lin, S. Y. Chen, *Inorg. Chem. Commun.*, 2011, **14**, 1588-1590.

17 (a) K. Liu, B. Li, Y. Li, X. Li, F. Yang, G. Zeng, Y. Peng, Z. Zhang, G. Li, Z. Shi, S. Feng and D. Song, *Chem. Commun.*, 2014, **50**, 5031-5033; (b) J. S. Qin, D. Y. Du, W. L. Li, J. P. Zhang, S. L. Li, Z. M. Su, X. L. Wang, Q. Xu, K. Z. Shao and Y. Q. Lan, *Chem. Sci.*, 2012, **3**, 2114-2118; (c) S. J. Bao, R. Krishna, Y. B. He, J. S. Qin, Z. M. Su, S. L. Li, W. Xie, D. Y. Du, W. W. He, S. R. Zhang and Y. Q. Lan, *J. Mater. Chem. A*, 2015, **3**, 7361-7367.

18 (a) P. L. Llewellyn, S. Bourrelly, C. Serre, A. Vimont, M. Daturi, L. Hamon, G. D. Weireld, J. S. Chang, D. Y. Hong, Y. K. Hwang, S. H. Jhung and G. Férey, *Langmuir*, 2008, **24**, 7245-7250; (b) J. Moellmer, A. Moeller, F. Dreisbach, R. Glaeser, R. Staudt, *Microporous Mesoporous Mater.*, 2011, **138**, 140-148; (c) S. K. Nune, P. K. Thallapally, A. Dohnalkova, C. Wang, J. Liu and G. J. Exarhos, *Chem. Commun.*, 2010, **46**, 4878-4880.

For Table of Contents Use Only

Synopsis

Two robust metal-organic frameworks with uncoordinated N atoms for CO_2 adsorption

Guo-Jian Ren, Yan-Qing Liu, Tong-Liang Hu* and Xian-He Bu

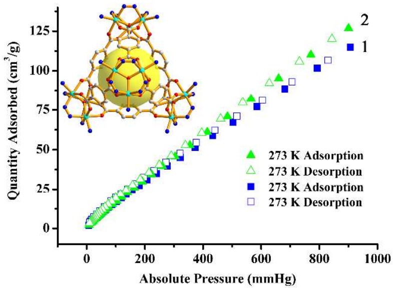

Two highly porous metal-organic frameworks are successfully constructed through the assembling of Co/Ni ions and mixed ligands. Contributed to uncoordinated tetrazolate N atoms of ligand, two complexes show high CO_2 adsorption capacities, serving as potential CO_2 adsorption materials.